



Tikrit Journal of Pharmaceutical Sciences

ISSN: 1815-2716 (print) -- ISSN: 2664-231X (online)

Journal Home Page: <https://tjphs.tu.edu.iq> -- Email: tjops@tu.edu.iq




Exploring Natural Medicinal Plants for Novel Bcl-2 Inhibitors: In Silico Drug Design and Computational Interaction Mechanism for Anti-Cancer Activity.

Riyadh Ahmed Atto AL-SHUAEEB¹, Ali Hussein Abbas², Mostafa Fayez Tawfeeq², Sattar Jabir Abood³

¹ Department of Pharmacy / Al-Qalam University College, Kirkuk 36001, Iraq.

² Department of Pharmaceutical Chemistry, College of Pharmacy, Tikrit University, Tikrit/Salah-Aldin, Iraq.

³ Department of Pharmacology and Toxicology, College of Pharmacy, Al Farahidi University, Baghdad, Iraq.

<p>Keywords: Bcl-2, Phytomolecules, Computational docking, IMPPAT database, ADMET, Molecular simulation.</p>	<p>Abstract The disturbance of typical cellular programmed cell death, known as apoptosis, constitutes a distinctive feature across all categories of malignancies. This maladjustment of apoptosis has the potential to result in diverse pathological states such as cancer, autoimmune illnesses, and neurodegenerative disorders. The regulation of apoptosis hinges upon proteins affiliated with the Bcl-2 family, which possess the capacity to either foster or impede this progression. The exaggerated expression of anti-apoptotic proteins (Bcl-2, Bcl-xL, and Mcl-1) has been linked to the sustenance, proliferation, and advancement of tumors. Lately, there has been a surge of interest in investigating small compounds and peptides that possess the ability to bind to the BH3 binding pocket of these proteins, as they exhibit promising potential as agents against cancer. Initially, the primary emphasis in the development of anti-cancer agents targeting this protein family was centered on suppressing Bcl-2. However, the precise mechanisms of drugs specific to Bcl-2 and their impacts have not been fully clarified through computational approaches. By conducting a molecular docking analysis against the Bcl-2 protein (PDB ID: 4LVT), out of the 8450 phytomolecules, 6742 compounds were effectively docked with Bcl-2, displaying docking scores ranging from -7.22 kcal/mol to +5.54 kcal/mol. Further investigation employing structure-based molecular docking (SB-MD) and ADMET (absorption, distribution, metabolism, excretion, and toxicity) profile analysis led to the identification of several plant-derived compounds, such as “Norepinephrine, Australine, Calystegine B, 7,7 A-Diepiealexine, and Alpha-Methylnoradrenaline” which exhibited strong binding to the active site residues of Bcl-2. In summary, these phytocompounds show promise as potential molecules against the Bcl-2 protein (4LVT) and warrant further validation through “<i>in vitro</i> and <i>in vivo</i>” experiments.</p>
<p>Article history: -Received: 14/02/2024 -Received in revised: 02/04/2024 -Accepted: 15/04/2024 -Available online: 25/06/2024</p>	
<p>*Corresponding author: Ali Hussain Abbas alih.phchm@tu.edu.iq</p>	
<p>© 2024 College of Pharmacy, Tikrit University. This is an open access article under the CC BY license https://creativecommons.org/licenses/by/4.0/</p> 	
<p>Citation: AL-SHUAEEB R.A.A., Abbas A.H. and Abood S.J. Exploring Natural Medicinal Plants for Novel Bcl-2 Inhibitors: In Silico Drug Design and Computational Interaction mechanism for Anti-Cancer Activity. Tikrit Journal of Pharmaceutical Sciences 2024; 18(1):1-11. http://doi.org/10.25130/tjphs.2024.18.1.1.1.11</p>	

استكشاف النباتات الطبية الطبيعية كمثبطات جديدة لـ Bcl-2 : تصميم دواء والية تداخل حسابي للنشاط المضاد للسرطان باستخدام بيئة الحاسوب

رياض احمد عطا الشعيب¹، علي حسين عباس²، مصطفى فايز توفيق²، ستار جابر عبود³

¹ قسم الصيدلة، كلية القام الجامعة، كركوك 36001، العراق
² فرع الكيمياء الصيدلانية، كلية الصيدلة، جامعة تكريت، تكريت/ صلاح الدين، العراق
³ فرع الادوية والسموم، كلية الصيدلة، جامعة الفراهيدي، بغداد، العراق

الخلاصة

يشكل اضطراب موت الخلايا المبرمج الخلوي النموذجي، والمعروف باسم موت الخلايا المبرمج، سمة مميزة لجميع فئات الأورام الخبيثة. هذا الخلل في موت الخلايا المبرمج لديه القدرة على أن يؤدي إلى حالات مرضية متنوعة مثل السرطان وأمراض المناعة الذاتية واضطرابات التنكس العصبي. يعتمد تنظيم موت الخلايا المبرمج على البروتينات المرتبطة بعائلة Bcl-2، والتي تمتلك القدرة على تعزيز أو إعاقة هذا التقدم. تم ربط التعبير المبالغ فيه عن البروتينات المضادة لموت الخلايا المبرمج (Bcl-2، Bcl-xL، و Mcl-1) بتغذية الأورام وانتشارها وتطورها. في الآونة الأخيرة، كان هناك زيادة في الاهتمام بدراسة المركبات الصغيرة والبيبتيدات التي تمتلك القدرة على الارتباط بجيب ربط BH3 لهذه البروتينات، حيث أنها تظهر إمكانات واعدة كعوامل ضد السرطان. في البداية، كان التركيز الأساسي في تطوير العوامل المضادة للسرطان التي تستهدف عائلة البروتين هذه يتركز على قمع Bcl-2. ومع ذلك، لم يتم توضيح الآليات الدقيقة للأدوية الخاصة بـ Bcl-2 وتأثيراتها بشكل كامل من خلال الأساليب الحسابية. من خلال تحليل الالتحام الجزيئي ضد بروتين Bcl-2 (معرف PDB: 4LVT)، من بين 8450 جزيئاً نباتياً، تم إرساء 6742 مركباً بشكل فعال مع Bcl-2، مما عرض درجات إرساء تتراوح من -7.22 كيلو كالوري/مول إلى +5.54 كيلو كالوري/مول. أدى المزيد من البحث باستخدام الالتحام الجزيئي القائم على البنية (SB-MD) وتحليل ملف ADMET (الامتصاص والتوزيع والتمثيل الغذائي والإفراز والسمية) إلى تحديد العديد من المركبات المشتقة من النبات، مثل "النوربينفرين، وأسترالين، وكاليسيتيجين ب، 7،7-دايبيلالكسين و الفا-مثيل نورادرينالين" اللذين أظهروا ارتباطاً قوياً ببقايا الموقع النشط لـ Bcl-2. باختصار، تظهر هذه المركبات النباتية فعالية واعدة كجزيئات محتملة ضد بروتين Bcl-2 (4LVT) وتستدعي المزيد من التحقق من الصحة من خلال التجارب "في المختبر وفي الجسم الحي".

الكلمات المفتاحية: Bcl-2؛ الجزيئات النباتية؛ الإرساء الحسابي؛ قاعدة بيانات IMPPAT؛ أدميت؛ المحاكاة الجزيئية.

Introduction:

Cancer is the result of a disturbance in the normal programmed cell death activity of dividing, living cells. Programmed cell death, known as apoptosis, is a tightly regulated and highly conserved process that eliminates aged or damaged cell, ⁽¹⁾ which is essential for cellular regulation and equilibrium, the extrinsic and intrinsic pathways (two well-regulated mechanisms) play a significant role in normal cellular conditions. ⁽²⁾ The extrinsic pathway relies on external factors like heat, radiation, and inadequate nourishment. Mitochondria controls the intrinsic pathway, ⁽³⁾ in which the Bcl-2 predominantly participates in this pathway and they have been extensively investigated as potential targets for diverse cancer treatments. ⁽⁴⁾ The Bcl-2 family encompasses both pro and anti-apoptotic proteins, with different Bcl proteins present in various regions of the human body. ⁽⁵⁾ There is association between anti-death proteins (Bcl-2, Bcl-XL, and Mcl-1) overexpression and tumor development, maintenance, and progression. ^(6,7) In all anti-death proteins the conserved Bcl-2 homology (BH) peptide domains-which involves 4 classes known as BH1, BH2, BH3, and BH4-are present. ⁽⁸⁾ BH3 is a 16-25 amino acid protein interaction motif predominantly found in pro-death members of the Bcl-2 protein family. ⁽⁹⁾ Peptides that bind to the BH3 domain attach to anti-death Bcl-2 proteins through a hydrophobic groove on their surface, promoting cellular demise. ⁽¹⁰⁾ The initial group of compounds investigated for Bcl-2 inhibition were peptides that imitated BH3-only proteins, exclusively targeting the

BH3 region of anti-death proteins. ⁽¹¹⁾ Peptidomimetic drugs were subsequently developed. Recently, clinical trials have been conducted on small molecule analogs of the amino acids involved in BH3 peptide binding interactions. ⁽¹²⁾ Drugs that bind to and hinder specific classes of Bcl-2 proteins have been also uncovered depending on fragment-based drug discovery and NMR-based structure prediction. "ABT-199 is a selective inhibitor of Bcl-2". ⁽¹³⁾ It is currently undergoing Phase III clinical trials, exhibiting >4800-fold greater selectivity (with a K_i of 0.01 nM) compared to other anti-apoptotic proteins such as Bcl-xL and Bcl-w, and it does not affect Mcl-1. Obatoclax is a broad-spectrum Bcl-2 antagonist ⁽¹⁴⁾, with average IC50 values of 3 mM and 2.9 mM on Mcl-1 and Bcl-2, respectively ⁽¹⁵⁾, it has successfully completed phase I and II clinical studies for various malignancies. ⁽¹⁶⁾ Molecules such as ABT-737 and its orally active derivative ABT-263 demonstrate binding affinity towards Bcl-2 and Bcl-xL proteins, while not interacting with Mcl-1. ⁽¹⁷⁾ Several plant extracts, including "clove, neem, oregano, garlic, turmeric, cinnamon", and various others, have previously exhibited inhibitory properties and have shown efficacy against *A. baumannii* and multiple drug-resistant strains, particularly in biofilm inhibition. ⁽¹⁸⁻²⁰⁾ Due to their reduced adverse effects and undesirable reactions compared to synthetic medications, phytochemicals are the preferred choice. Consequently, it is crucial to test potent phytochemicals derived from medicinal sources

against pathogenic bacterial proteins like ASPP2(Ank-SH3) to facilitate the development of novel and safe antimicrobial drugs.^(21, 22) Bcl-2 was selected as targets in this research due to its prevalence in most cancer types.

Notably, Bcl-2 now possesses a well-defined three-dimensional crystal structure (PDB ID: 4LVT). To identify natural lead-like phytochemicals against the *Acinetobacter baumannii* response regulator “BfmR” enzyme and examine its molecular dynamics, a bioinformatics-driven hierarchy to search the IMPPAT database was employed.⁽²³⁾ Subsequently, molecular dynamics simulations (MDS)⁽²⁴⁾ were conducted to validate the binding affinity of the most promising phytochemical inhibitors within the BfmR active pocket. These inhibitors include “Norepinephrine, Australine, Calystegine B, 7,7 A-Diepialexine, and Alpha-Methylnoradrenaline”.

Materials and Methods

1-Selection and preparation of ligands from the IMPPAT database

The Plant Phytochemicals Database (IMPPAT) is a repository for phytochemicals found in plants. Herbs from India gathered to find a ligand library for this study depending on the details in IMPPAT of 14,011 phytochemicals.⁽²⁵⁾ As a result, the most widely utilized Lipinski's rule of five (Ro5), a drug-like filter, was used to screen the ligand library's potential drug-like compounds. There were 8,450 out of 14, 011 which were passed Ro5 (drug-like filter). After that, the three-dimensional Structure Data File was downloaded (3-D SDF). The IMPPAT database provided the structure of these phytochemicals. Venetoclax and navitoclax are FDA-approved medications used as reference compounds in this study.

2-Preparation of protein

To conduct docking studies, the resolved crystal structure of the apoptosis regulator Bcl-2 (PDB ID: 4LVT) from the Protein Data Bank (PDB) website (www.rcsb.org) was obtained.⁽²⁶⁾ Prior to the docking analysis, the 3D crystal structure underwent necessary preparations, including the removal of water molecules and HETATM from the published structures. The energy minimization process employed the CHARMM force field, utilizing Discovery Studio Visualizer 2019. Furthermore, the active site of the pre-bound ligand molecules present in both structures was analyzed. All atoms and bonds within a 5\AA radius of the selection zone was selected and the relevant amino acid residue information from the active site was collected. This information was then utilized to perform docking analysis on the corresponding binding pocket.

3-Molecular docking/ protocol

By performing molecular docking analysis, the inhibitory effects of all the investigated compounds against the 4LVT protein was evaluated. The protocol described in references 27 and 28 was followed.

A-Molecular docking protocol validation

To validate the docking protocol, we excluded the coordinates of the bound ligand inhibitor IXJ from the

crystal complex of 4LVT and verified the bond orders. The protocol described in reference 28 was followed.

B-Pharmacoinformatics analysis

To ensure the comprehensive analysis of selected and newly designed compounds, we employed several pharmacoinformatics tools. The details described in reference 29.

C-Molecular Dynamic Simulation

To evaluate the stability of the protein backbone within the docking complex, we conducted a molecular dynamics simulation experiment using GROMACS version 2019.4⁽²⁸⁾. The Gromos54a7 all-atom force field⁽³⁰⁾ was employed for the simulation. The complexes with the lowest binding energies, as determined from the molecular docking analysis, were subjected to the simulation. For explicit solvation in the molecular dynamics (MD) simulations, we selected the SPC water model.⁽³¹⁾ The dimensions of the rectangular box, ensuring a minimum separation of 1 nm between any atom and the box boundary to satisfy periodic boundary conditions, were determined to be 8.19 nm x 8.76 nm x 8.12 nm. The ProDRG webserver was used as source to obtain charge parameters for the ligand.⁽³²⁾ To balance the system's charge, Na^+ and Cl^- atoms were introduced into the solution. The energy minimization process employed the steepest descent algorithm, with a maximum force (Fmax) threshold set at 1000 kJ/mol.nm. Subsequently, the system underwent equilibration at a temperature of 300 K and pressure of 1 bar, accomplished by conducting two consecutive 100 ps simulations using the canonical NVT and isobaric NPT ensembles, respectively. Throughout the equilibration phase, both the protein and docked ligands were independently restrained, and thermostat coupling was applied for the entire simulation. The MD simulations were run for 100 ns with stable temperature and pressure, utilizing a time step of 2 fs and a long-range interaction cut-off of 1 nm. Trajectory analysis was performed using GROMACS tools to extract relevant information from the simulations.

D-Binding free energy calculation

The binding free energy of each protein-ligand complex was determined using the MM/GBSA (Molecular Mechanics/Generalized Born Surface Area) approach based on the MD simulation trajectories. The `gmx_MMPBSA` package was employed for the calculations, utilizing snapshots extracted from the production MD trajectory at an interval of 100 ps from the 80-100 ns timeframe.^(26,32) The calculation focused on evaluating the free energy (ΔG_{bind}) associated with the formation of the ligand-receptor complex. The calculation done by equations described in references 28 and 33. In the MM/GBSA (Molecular Mechanics/Generalized Born Surface Area) approach various energy components-including “changes in the gas phase molecular mechanics energy (ΔE_{MM}), solvation free energy (ΔG_{solv}), and conformational entropy ($-T\Delta S$)” upon ligand binding-were considered to determine the binding free energy (ΔG_{bind}). Fixed geometries before and after binding was obtained by cancelling out the bonded internal energy terms (ΔE_{bond} , ΔE_{angle} , and $\Delta E_{dihedral}$). The

nonbonded Van der Waals interaction energy (ΔE_{vdW}) and electrostatic interaction energy (ΔE_{ele}) are also taken into account. The solvation free energy (ΔG_{solv}) is composed of two components. The “polar contribution (ΔG_{GB})” is calculated using the “GB-OBC1” model, which considers the electrostatic solvation energy. To account for the nonpolar interactions between the solute and the continuum solvent, the “solvent-accessible surface area (SASA)” used for estimation the nonpolar contribution (ΔG_{SA}).⁽³⁴⁾

Results and Discussion

1-Molecular docking analysis

Table 1 presents the binding affinity of all studied compounds, including “Norepinephrine, Australine, Calystegine B, 7,7 A-Diepilexine, and Alpha-Methylnoradrenaline” against the 4LVT receptor. The maximum binding affinity of the ligands indicated by lowest binding energy (most negative). The two-dimensional (2D) binding modes of the complexes formed between the studied compounds and 4LVT are summarized in Figures 1. The results in Table 1 highlight that “7,7 A-Diepilexine, Alpha-

Methylnoradrenaline, and Norepinephrine” exhibit the highest binding affinity within the 4LVT receptor compared to the other compounds. Figure 1 illustrates the binding interactions of Alpha-Methylnoradrenaline (binding affinity-8.92 kcal/mol) with Glu142 and Ala97 residues in 4LVT through three hydrogen bonds. Additionally, Ala146, Tyr105, Leu198, Tyr199, and Trp141 residues in 4LVT participate in binding interactions with Alpha-Methylnoradrenaline through Van der Waals interactions. Moreover, 7,7 A-Diepilexine (binding affinity -8.40 kcal/mol) forms a hydrogen bond with Ala97 residue in 4LVT, and binding interactions with Ala146, Tyr199, Val145, and Asp100 residues in 4LVT occur through Van der Waals interactions. Furthermore, Norepinephrine (binding affinity -7.80 kcal/mol) engages in binding interactions with Leu198, Tyr199, Phe195, Asp100, Tyr105, and Glu142 residues in 4LVT through two hydrogen bonds. In addition, Met82, Leu35, Val66, and Val20 residues in 4LVT participate in binding interactions with Norepinephrine through Van der Waals interactions, as shown in Figure 1.

Table 1: The affinity of binding against 4LVT of all compounds in this study

Comp.	Docking Score (kcal/mol)
Norepinephrine	-7.80
Australine	-7.60
Calystegine B	-7.56
7,7 A-Diepilexine	-8.40
Alpha-Methylnoradrenaline	-8.92
IXJ	-7.70

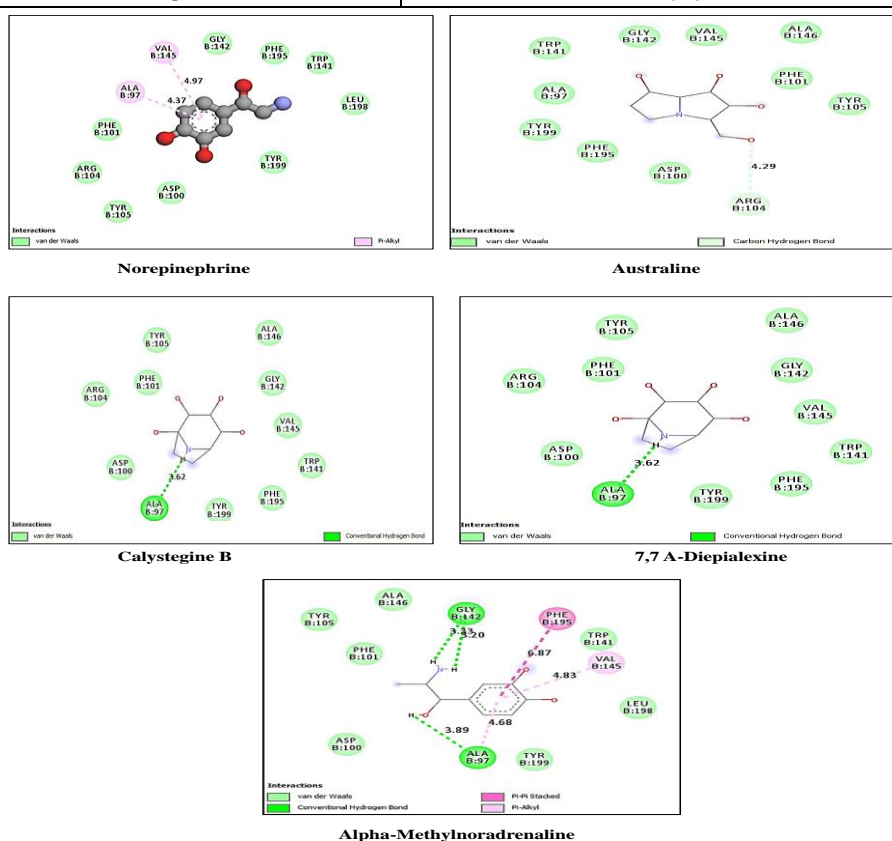


Fig. 1: complexes of some studied compounds inside 4LVT (2D binding modes)

2-Pharmacoinformatic studies

Table 2 presents the results of the Drug Score and Drug Likeness model for the investigated compounds. It is crucial to acknowledge that compounds displaying zero or negative values should not be regarded as suitable candidates for drug-like properties. Among the analyzed compounds, Alpha-Methylnoradrenaline demonstrated the highest scores for both Drug Score and Drug Likeness, achieving values of 1.17. Subsequently, 7,7 A-Diepialexine and Norepinephrine obtained Drug Likeness scores of 1.15 and 1.07, respectively. These findings imply that these three compounds exhibit significant potential for further development as drug leads.

Table 3 presents a summary of the descriptors for molecular properties of the compounds investigated, based on "Lipinski's Rules of Five". The calculations and theoretical framework for these descriptors were carried out following a previous study.⁽³⁵⁾ "Lipinski's Rules of Five" are extensively utilized in the field of drug development and design to predict the oral bioavailability of drug molecules. "Lipinski's rule" encompasses five criteria used to assess the potential of a compound to function as an orally active drug. According to these guidelines, a compound intended for oral activity should obey the following criteria: (i) molecule's lipophilicity measured by log P value should not exceed five. (ii) The molecular weight (MW) should be less than 500 Da. (iii) The number of hydrogen bond donors (nON) should not surpass five. (iv) The number of hydrogen bond acceptors (nOHN) should not surpass ten. (v) The topological polar surface area (TPSA) should be below 160 Å and should not violate more than one of them. As presented in Table 3, none of the compounds studied violated any of

"Lipinski's Rules of Five", indicating their potential as orally active drugs.

Tables 4 and 5 provide a comprehensive overview of the ADMET properties, encompassing absorption, distribution, metabolism, excretion, and toxicity, for the compounds investigated. The ADMET profiles offer valuable insights into the potential of these compounds as drug candidates. The utilized database incorporates diverse ADMET characteristics that evaluate the capacity of the studied compounds to serve as drug leads. These characteristics include the penetration of the blood-brain barrier (BBB), human intestinal absorption (HIA), permeability across Caco-2 cells, CYP inhibitory promiscuity, AMES toxicity, carcinogenicity, and acute toxicity LD50 in rats. The outcomes of these evaluations are presented in Tables 4 and 5. As evidenced in Tables 4 and 5, all the examined compounds demonstrate BBB permeability and absorption in the human intestine (HIA) furthermore, notable permeability for Caco-2 cells was observed, particularly for Isoliensinine, Liensinine, and Methylcorypalline. Notably, these compounds were found to have a favorable metabolic profile, as they were identified as non-substrates and non-inhibitors of CYP enzymes.⁽³³⁾ In terms of AMES toxicity, none of the studied compounds exhibited toxic effects. The carcinogenicity model also indicated the absence of carcinogenic properties in these compounds. Moreover, the rat acute toxicity LD50 values for all the compounds fell within the range of 2.10 to 3.19 mol/kg. The comprehensive information provided in Tables 4 and 5 strongly supports the potential of these investigated compounds as viable drug candidates, given their desirable ADMET properties.

Table 2: Drug score and drug similarity index

Comp.	Drug score	Drug similarity
Norepinephrine	1.07	7.43
Australine	0.67	2.54
Calystegine B	0.83	5.46
7,7 A-Diepialexine	1.15	7.84
Alpha-Methylnoradrenaline	1.17	8.54

Table 3: Descriptors of molecular properties

Comp.	Molecular weight	Partition coefficient in logarithmic scale	Number of Rotatable Bonds	Hydrogen bond Numbers as Acceptors	Hydrogen bond Numbers as donors	Polar surface area	Water solubility (log mol/L)
Norepinephrine	169.18	2.58	2	5	3	134.92	-2.81
Australine	189.21	2.53	3	4	3	123.56	-2.80
Calystegine B	175.18	2.82	0	3	1	117.07	-3.30
7,7 A-Diepialexine	189.21	3.18	4	4	1	136.82	-3.20
Alpha-Methylnoradrenaline	183.21	4	2	3	0	129.60	-5.14

Table 4: ADMET properties (Cont.)

Comp.	Caco2 permeability	Intestinal absorption	Skin Permeability	P-glycoprotein substrate	P-glycoprotein substrate	P-glycoprotein I inhibitor	VD _{ss} (human)	Fraction unbound (human)
Norepinephrine	1.024	89.132	-2.758	Yes	No	No	1.41	0.385
Australine	1.19	88.84	-3.17	Yes	No	No	1.11	0.331
Calystegine B	1.27	98.08	-2.60	No	No	No	1.17	0.17
7,7 A-Diepialexine	1.38	89.79	-3.11	No	Yes	No	1.11	0.23
Alpha-Methylnoradrenaline	1.28	98.69	-2.36	No	Yes	Yes	0.61	0.05

Table 5: ADMET properties

Comp.	BBB	CYP2D6 substrate	CYP3A4 substrate	CYP1A2 inhibitor	AMES toxicity	Oral Toxicity (LD50)	Hepatotoxicity	Skin Sensitization
Norepinephrine	-0.70	No	No	Yes	No	2.44	No	No
Australine	0.07	No	Yes	Yes	No	2.55	Yes	No
Calystegine B	0.30	No	Yes	No	No	2.89	Yes	No
7,7 A-Diepialexine	1.38	No	Yes	No	No	3.19	Yes	No
Alpha-Methylnoradrenaline	0.26	No	Yes	No	Yes	2.52	No	No

3-Molecular dynamic simulation

To evaluate the stability of the docked complexes and examine the protein backbone stability within the docking complex, molecular dynamics simulations were conducted. Specifically, simulations were executed on the 4LVT protein in two distinct scenarios: in the absence of any ligand and in the presence of three particular ligands, namely "7,7 A-Diepialexine, Alpha-Methylnoradrenaline, and Norepinephrine". The simulations spanned a duration of 100 ns and employed an explicit solvation system. Additionally, to mimic physiological conditions, a physiological salt concentration was maintained throughout the simulations.

4-The root means square deviation (RMSD)

To assess the stability of the protein backbone in the presence and absence of ligands, the Root Mean Square Deviation (RMSD) values were calculated during the course of molecular dynamics simulations. As depicted in Figure 2, the RMSD values for the protein backbone demonstrated stabilization after 5 ns of simulation.

These values indicated comparable changes in the conformation of the protein backbone compared to the initial structures, with values below 0.50 nm. Notably, the apo-form of 4LVT exhibited the highest deviation in RMSD values, whereas the docked ligands, such as "7,7 A-Diepialexine, Alpha-Methylnoradrenaline, and Norepinephrine", displayed similar or lower RMSD values. This observation suggests that the docked ligands contribute to the stabilization of the 4LVT structure to some extent. The average RMSD values for the final 10 ns of the simulation were 0.34 ± 0.09 nm for 4LVT, 0.30 ± 0.11 nm for Alpha-Methylnoradrenaline within 4LVT, 0.29 ± 0.07 nm for 7,7 A-Diepialexine within 4LVT, and 0.26 ± 0.10 nm for Norepinephrine within 4LVT, respectively.

5-Root mean square fluctuation (RMSF)

The mobility and flexibility of protein residues during the simulation were analyzed by calculating the Root Mean Square Fluctuation (RMSF) values at the residue level. Figure 3 displays the RMSF values for the 4LVT protein both with and without ligands, including 7,7 A-Diepialexine, Alpha-Methylnoradrenaline, and Norepinephrine. As expected, the terminal residues of

4LVT and the docked ligands exhibited higher RMSF values, indicating their greater mobility. Specifically, in the apo-4LVT structure bound to 7,7 A-Diepialexine, residues 40 and 45 showed increased mobility. In the case of the apo-4LVT structure bound to Alpha-Methylnoradrenaline, residues 45, 55, and 70 exhibited higher flexibility. Additionally, the binding of Norepinephrine to 4LVT resulted in higher flexibility in residues 26-28.

These variations in RMSF values among different residues suggest differences in the binding characteristics of each ligand and their subsequent influence on protein structure and dynamics. Although Figure 3 shows similar RMSF values overall, specific residue-level changes can be observed upon binding of different ligands.

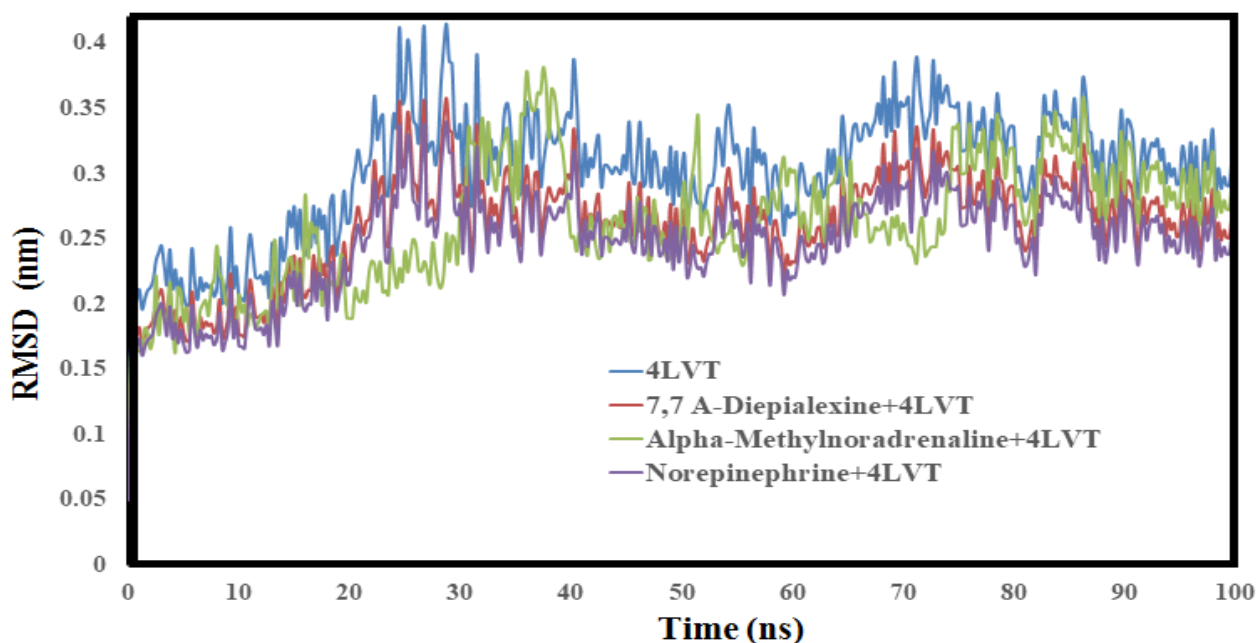


Fig. 2: “RMSD values of the protein backbone with or without ligands, 7,7 A-Diepialexine, Alpha-Methylnoradrenaline and Norepinephrine

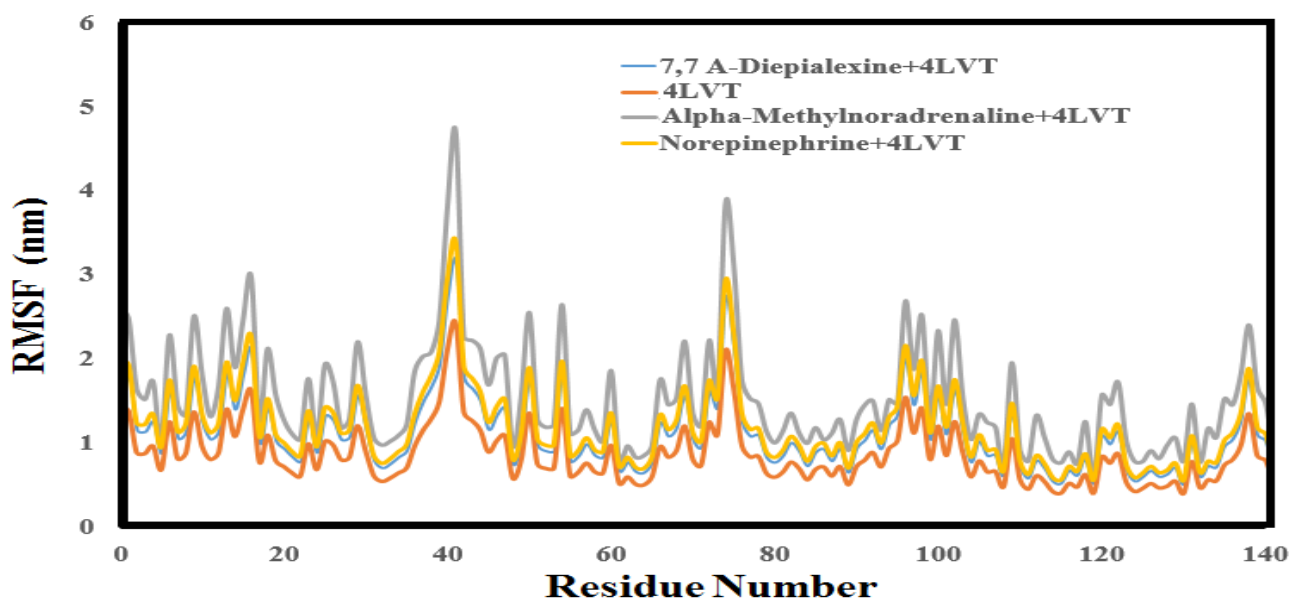


Fig. 3: “RMSF values of the 4LVT with and 7,7 A-Diepialexine, Alpha-Methylnoradrenaline and Norepinephrine ligands”.

6-Radius of gyration (Rg)

To evaluate the overall impact of the ligands on the structure of 4LVT, the radius of gyration (Rg) values was computed for each complex, and the outcomes are depicted in Figure 4. The Rg values for the apo-4LVT and the 4LVT complexes with 7,7 A-Diepiealexine, Alpha-Methylnoradrenaline, and Norepinephrine were determined to be (2.29, 2.27, 2.26, and 2.23) nm, respectively. Because Norepinephrine exhibits the lowest Rg value among the ligands this indicate that the protease structure when bound with becomes more compact when bound with Norepinephrine.

7-Hydrogen bonds (H-bonds) counts

The number of hydrogen bonds formed between main protein (4LVT: which is a potent lymphoid tyrosine phosphatase inhibitor in T cells) and the ligands can insights into the variations in the binding patterns of different ligands with the main protein, as well as the nature of their interactions.

Figure 5 illustrates the number of hydrogen bonds formed by the protease with “7,7 A-Diepiealexine, Alpha-Methylnoradrenaline, and Norepinephrine” during the simulation. It is evident that 7,7 A-Diepiealexine forms a greater number of hydrogen bonds compared to the other compounds. The average number of hydrogen bonds formed between 4LVT and the ligands “7,7 A-Diepiealexine, Alpha-Methylnoradrenaline, and Norepinephrine” over the course of the 100 ns simulation, comprising 100,000 time points, were found to be 3.25, 3.15, and 2.99, respectively. Hydrogen bonds formed in an aqueous solution differs significantly for all four ligands in spite of similar should be binding energies exhibited by the docked complexes. This disparity can likely be attributed to the absence of solvent in the docking process, as the solvent environment can profoundly influence ligand binding.

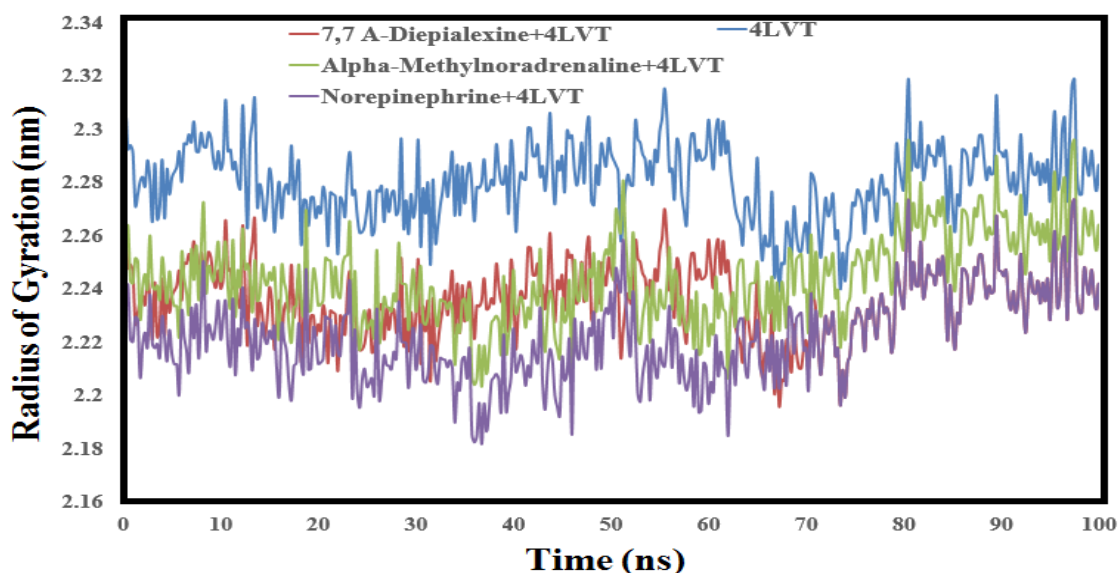


Fig. 4. “Radius of Gyration (Rg) analysis shows that each ligand induces compactness to the 4LVT structure; however, binding of Norepinephrine demonstrated the most compact structure”.

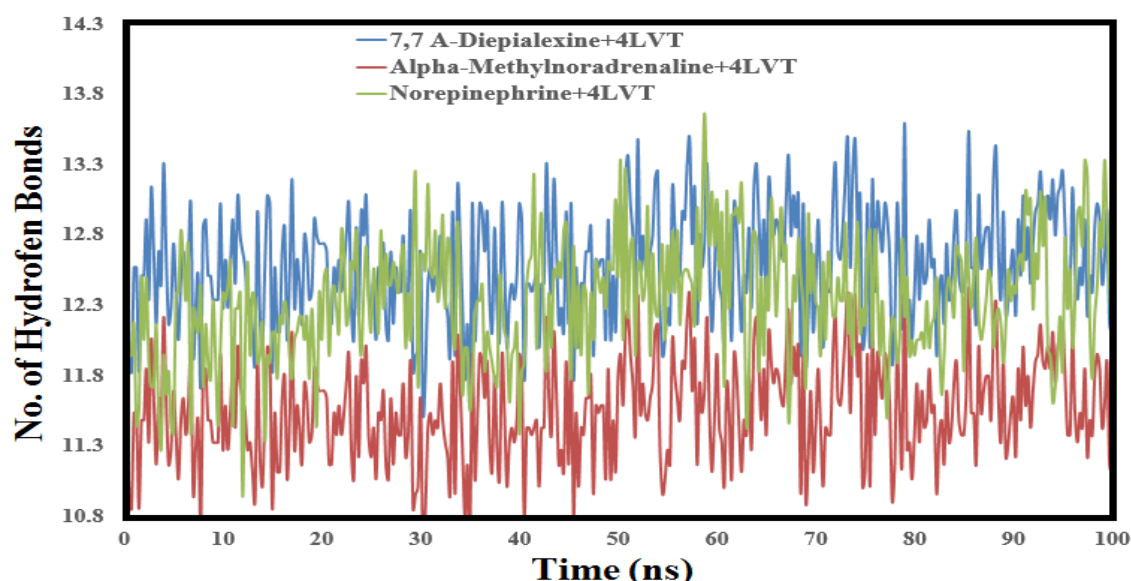


Fig. 5. “Number of hydrogen bonds formed during the course of simulation by the 4LVT with the 7,7 A-Diepiealexine, Alpha-Methylnoradrenaline and Norepinephrine”.

8-Protein-ligand interaction energy/ analysis

Apart from molecular dynamics simulations, the MM/GBSA method was utilized to compute the binding free energies of the top three hit compounds, utilizing data obtained from the final 80 ns of the 100 ns MD simulation trajectories. The MM/GBSA analysis is a commonly employed technique for estimating interaction energies, which leverages molecular dynamics simulation trajectories to predict the binding free energies (ΔG_{bind}) of protein-ligand systems. The calculated ΔG_{bind} values for the ligands remained negative, indicating favorable binding, as demonstrated in Table 6.

Among the investigated compounds “7,7 A-Diepialexine” exhibited a consistently negative mean value of -33.90 ± 7.16 for the binding free energy, surpassing the other compounds. This suggests that nonpolar interaction energy plays a significant role in the binding process, emphasizing the importance of hydrophobic interactions between “7,7 A-Diepialexine” and 4LVT. The negative electrostatic energy indicates the presence of favorable intermolecular hydrogen bonds. It is noteworthy that in all three studied systems (4LVT-“7,7-A-Diepialexine”, 4LVT-“Alpha-Methylnoradrenaline”, and 4LVT-“Norepinephrine”), the polar solvation energy opposes the binding, but this is counterbalanced by favorable van der Waals energy, electrostatics energy, and nonpolar solvation energy.

Table 6. MMPBSA energy (ΔE_{MMPBSA}) studies

Criteria In (kcal/mol)	4LVT-7,7 A-Diepialexine	4LVT- Alpha-Methylnoradrenaline	4LVT- Norepinephrine
ΔE_{vdW}	-27.84 ± 3.49	-25.62 ± 2.08	-18.45 ± 3.53
ΔE_{elec}	-530.98 ± 34.32	-415.10 ± 29.14	-235.89 ± 18.87
ΔG_{GB}	531.08 ± 36.39	415.45 ± 30.27	235.96 ± 10.34
ΔG_{SA}	-6.23 ± 2.37	-5.48 ± 3.15	-4.32 ± 2.98
ΔG_{gas}	-545.25 ± 32.06	-341.95 ± 28.37	-257.39 ± 16.43
ΔG_{Solv}	545.32 ± 31.97	342.00 ± 23.91	260.23 ± 19.44
ΔG_{bind}	-33.90 ± 7.16	-30.7 ± 5.16	-19.86 ± 3.19

Conclusion

Through molecular docking, significant binding potential of “Norepinephrine, Australine, Calystegine B, 7,7 A-Diepialexine, and Alpha-Methylnoradrenaline” to the 4LVT protein compared to FDA approved drugs was observed. Molecular docking simulations further revealed strong binding of “7,7 A-Diepialexine, Alpha-Methylnoradrenaline, and Norepinephrine” which stabilize the structure of 4LVT by forming stable complexes. These findings suggest that 4LVT can serve as a potential target for novel drug development using “7,7 A-Diepialexine, Alpha-Methylnoradrenaline, and Norepinephrine” as promising lead phytocompounds. Experimental validation through in vitro and in vivo studies can be conducted to explore their potential for drug discovery against *A. baumannii*. Lipinski’s rule was established based on five rules to compute the ability of the compound to act as an orally active drug. According to Lipinski’s rule, the orally active drug must have no

more than one violation of the following standards: (i) octanol/water partition coefficient ($\log P$), which measured the lipophilicity of a molecule must be not greater than five; (ii) a molecular weight (MW) less than 500 Da; (iii) not more than five hydrogen bond donors (nOHNH); (iv) not more than 10 hydrogen bond acceptors (nON); and (v) topological polar surface area (TPSA) below the limit of 160 Å. (36) So, Compounds with higher weights are less likely to be absorbed and therefore to ever reach the place of action. (37, 38) If we apply the molecular weight pillar on our compounds, we can say all studied compounds are obey Lipinski’s rule.

Conflict of interest

The author(s) declare no conflict of interest, financial or otherwise.

References

- Acoca S, Cui Q, Shore GC, Purisima EO. Molecular dynamics study of small molecule inhibitors of the Bcl-2 family. *Proteins: Structure, Function, and Bioinformatics*. 2011;79(9):2624-36
- dams JM, Cory S. The Bcl-2 apoptotic switch in cancer development and therapy. *Oncogene*. 2007;26(9):1324-37.
- Apoptosis Interest Group. (1999). About apoptosis. Archived from the original on 28 December 2006. Retrieved 2006-12-15.
- Ashkenazi A, Dixit VM. Death receptors: signaling and modulation. *science*. 1998;281(5381):1305-8.
- Ashkenazi A, Fairbrother WJ, Levenson JD, Souers AJ. From basic apoptosis discoveries to advanced selective Bcl-2 family inhibitors. *Nature reviews drug discovery*. 2017;16(4):273-84.
- Bernardo PH, Sivaraman T, Wan KF, Xu J, Krishnamoorthy J, Song CM, Tian L, Chin JS, Lim DS, Mok HY, Yu VC. Structural insights into the design of small molecule inhibitors that selectively antagonize Mcl-1. *Journal of medicinal chemistry*. 2010;53(5):2314-8.
- Bogenberger JM, Kornblau SM, Pierceall WE, Lena R, Chow D, Shi CX, Mantei J, Ahmann G, Gonzales IM, Choudhary A, Valdez R. Bcl-2 family proteins as 5-Azacytidine-sensitizing targets and determinants of response in myeloid malignancies. *Leukemia*. 2014;28(8):1657-65.
- Chen Y, Wang J, Zhang J, Wang W. Binding modes of Bcl-2 homology 3 (BH3) peptides with anti-apoptotic protein A1 and redesign of peptide inhibitors: a computational study. *Journal of Biomolecular Structure and Dynamics*. 2018;36(15):3967-77.
- Conus S, Kaufmann T, Fellay I, Otter I, Rossé T, Borner C. Bcl-2 is a monomeric protein: prevention of homodimerization by structural constraints. *The EMBO Journal*. 2000;19(7):1534-44.
- Cuconati A, Mukherjee C, Perez D, White E. DNA damage response and MCL-1 destruction initiate apoptosis in adenovirus-infected cells. *Genes & development*. 2003;17(23):2922-32.
- Czabotar PE, Lee EF, van Delft MF, Day CL, Smith BJ, Huang DC, Fairlie WD, Hinds MG, Colman PM. Structural insights into the degradation of Mcl-1 induced by BH3 domains. *Proceedings of the National Academy of Sciences*. 2007;104(15):6217-22.
- Dalafave DS, Prisco G. Inhibition of antiapoptotic Bcl-XL, Bcl-2, and MCL-1 proteins by small molecule mimetics. *Cancer informatics*. 2010;9:CIN-S5065.
- Doi K, Li R, Sung SS, Wu H, Liu Y, Manieri W, Krishnegowda G, Awwad A, Dewey A, Liu X, Amin S. Discovery of marinopyrrole A (maritoclax) as a selective Mcl-1 antagonist that overcomes ABT-737 resistance by binding to and targeting Mcl-1 for proteasomal degradation. *Journal of Biological Chemistry*. 2012;287(13):10224-35.
- Friberg A, Vigil D, Zhao B, Daniels RN, Burke JP, Garcia-Barrantes PM, Camper D, Chauder BA, Lee T, Olejniczak ET, Fesik SW. Discovery of potent myeloid cell leukemia 1 (Mcl-1) inhibitors using fragment-based methods and structure-based design. *Journal of medicinal chemistry*. 2013;56(1):15-30.
- Gregoli PA, Bondurant MC. The roles of Bcl-XL and apolipoprotein A1 in the control of erythropoiesis by erythropoietin. *Blood, The Journal of the American Society of Hematology*. 1997;90(2):630-40.
- Hafid-Medheb K, Augery-Bourget Y, Minatchy MN, Hanania N, Robert-Lézénès J. Bcl-XL is required for heme synthesis during the chemical induction of erythroid differentiation of murine erythroleukemia cells independently of its antiapoptotic function. *Blood, The Journal of the American Society of Hematology*. 2003;101(7):2575-83.
- Lokhande KB, Doiphode S, Vyas R, Swamy KV. Molecular docking and simulation studies on SARS-CoV-2 Mpro reveals Mitoxantrone, Leucovorin, Birinapant, and Dynasore as potent drugs against COVID-19. *Journal of Biomolecular Structure and Dynamics*. 2021;39(18):7294-305.
- Lokhande KB, Ghosh P, Nagar S, Venkateswara Swamy K. Novel B, C-ring truncated deguelin derivatives reveals as potential inhibitors of cyclin D1 and cyclin E using molecular docking and molecular dynamic simulation. *Molecular diversity*. 2021:1-5.
- Shahryari S, Mohammadnejad P, Noghabi KA. Screening of anti-Acinetobacter baumannii phytochemicals, based on the potential inhibitory effect on OmpA and OmpW functions. *Royal Society Open Science*. 2021;8(8):201652.
- Singh R, Bhardwaj VK, Sharma J, Das P, Purohit R. Discovery and in silico evaluation of aminoarylbenzosuberene molecules as novel checkpoint kinase 1 inhibitor determinants. *Genomics*. 2021;113(1):707-15.
- Katz C, Benyamini H, Rotem S, Lebendiker M, Danieli T, Iosub A, Refaely H, Dines M, Bronner V, Bravman T, Shalev DE. Molecular basis of the interaction between the antiapoptotic Bcl-2 family proteins and the proapoptotic protein ASPP2. *Proceedings of the National Academy of Sciences*. 2008;105(34):12277-82.
- Kelekar A, Thompson CB. Bcl-2-family proteins: the role of the BH3 domain in apoptosis. *Trends in cell biology*. 1998;8(8):324-30.
- Ku B, Liang C, Jung JU, Oh BH. Evidence that inhibition of BAX activation by Bcl-2 involves its tight and preferential interaction with the BH3 domain of BAX. *Cell research*. 2011;21(4):627-41.
- Kundaikar HS, Degani MS. Insights into the Interaction mechanism of ligands with Aβ42 based on molecular dynamics simulations and mechanics: implications of role of common binding site in drug design for Alzheimer's disease. *Chemical biology & drug design*. 2015;86(4):805-12.
- Mohanraj K, Karthikeyan BS, Vivek-Ananth RP, Chand RB, Aparna SR, Mangalapandi P, Samal A. IMPPAT: A curated database of Indian Medicinal Plants, Phytochemistry and Therapeutics. *Scientific reports*. 2018;8(1):4329.
- Martínez L, Andrade R, Birgin EG, Martínez JM. PACKMOL: A package for building initial configurations for molecular dynamics simulations.

Journal of computational chemistry. 2009;30(13):2157-64.

27. Mohammad T, Siddiqui S, Shamsi A, Alajmi MF, Hussain A, Islam A, Ahmad F, Hassan MI. Virtual screening approach to identify high-affinity inhibitors of serum and glucocorticoid-regulated kinase 1 among bioactive natural products: Combined molecular docking and simulation studies. *Molecules*. 2020;25(4):823.

28. Ahmed Atto Al-Shuaeeb R, Abd El-Mageed HR, Ahmed S, Mohamed HS, Hamza ZS, Rafi MO, Ahmad I, Patel H. In silico investigation and potential therapeutic approaches of isoquinoline alkaloids for neurodegenerative diseases: computer-aided drug design perspective. *Journal of Biomolecular Structure and Dynamics*. 2023:1-3

29. Sack JS, Gao M, Kiefer SE, Myers JE, Newitt JA, Wu S, Yan C. Crystal structure of microtubule affinity-regulating kinase 4 catalytic domain in complex with a pyrazolopyrimidine inhibitor. *Acta Crystallographica Section F: Structural Biology Communications*. 2016;72(2):129-34.

30. Kar RK, Suryadevara P, Sahoo BR, Sahoo GC, Dikhit MR, Das P. Exploring novel KDR inhibitors based on pharmaco-informatics methodology. *SAR and QSAR in Environmental Research*. 2013;24(3):215-34.

31. Schmid N, Eichenberger AP, Choutko A, Riniker S, Winger M, Mark AE, Van Gunsteren WF. Definition and testing of the GROMOS force-field versions 54A7 and 54B7. *European biophysics journal*. 2011;40:843-56.

32. Schüttelkopf AW, Van Aalten DM. PRODRG: a tool for high-throughput crystallography of protein-ligand complexes. *Acta Crystallographica Section D: Biological Crystallography*. 2004;60(8):1355-63.

33. Baker NA, Sept D, Joseph S, Holst MJ, McCammon JA. Electrostatics of nanosystems: application to microtubules and the ribosome. *Proceedings of the National Academy of Sciences*. 2001;98(18):10037-41.

34. Kumari R, Kumar R, Open Source Drug Discovery Consortium, Lynn A. g_mmpbsa • A GROMACS tool for high-throughput MM-PBSA calculations. *Journal of chemical information and modeling*. 2014;54(7):1951-62.

35. Ahmed SA, Rahman AA, Elsayed KN, Abd El-Mageed HR, Mohamed HS, Ahmed SA. Cytotoxic activity, molecular docking, pharmacokinetic properties and quantum mechanics calculations of the brown macroalga *Cystoseira trinodis* compounds. *Journal of Biomolecular Structure and Dynamics*. 2021;39(11):3855-73.

36. Ahmed Atto Al-Shuaeeb R, Abd El-Mageed HR, Ahmed S, Mohamed HS, Hamza ZS, Rafi MO, Ahmad I, Patel H. In silico investigation and potential therapeutic approaches of isoquinoline alkaloids for neurodegenerative diseases: Computer-aided drug design perspective. *Journal of Biomolecular Structure and Dynamics*. 2023;41(23):14484-14496.

37. Ahmed SA, Abdelrheem DA, El-Mageed HA, Mohamed HS, Rahman AA, Elsayed KN, Ahmed SA. Destabilizing the structural integrity of COVID-19 by caulerpin and its derivatives along with some antiviral drugs: an in silico approaches for a combination therapy. *Structural Chemistry*. 2020;31:2391-412.

38. Bensaad MS, Kahoul MA, Khier M, Mitra D, Benhoula M, Banjer HJ, Al-Eisa RA, Algehainy NA, Helal M, Al-Mushhin AA, Sami R. An Insight-Based Computational Approaches to Estimate Molecular Weight Distribution, Allergenicity and Immunological Aspects, Toxicity Profile, Possible Biodegradation, Persistence and Bioaccumulation Factor of Four Phyto-Compounds. *Journal of Biobased M*.